Influence of the Synthesis Conditions of Reduced Graphene Oxide on the Electrochemical Characteristics of the Oxygen Electrode

M.O. Danilov[1,*], I.A. Slobodyanyuk[1], I.A. Rusetskii[1], G.I. Dovbeshko[2], G.Ya. Kolbasov[1]

[1]Vernadskii Institute of General & Inorganic Chemistry of Nat. Acad. Sci., Kyiv, Ukraine
[2]Institute of Physics Nat. Acad. Sci., Kyiv, Ukraine
*Corresponding author: danilovmickle@rambler.ru

Abstract   Reduced graphene oxide (RGO) was obtained by chemical synthesis from multi walled carbon nanotubes. Using a suitable oxidant, we longitudinally "unzipped" nanotubes to form graphene oxide nanoribbons and then obtained RGO with a proper reductant. Standard redox potentials of carboxy groups were used for choosing oxidant and reductant. It has been shown that the required oxidant potential in acid medium should be more + 0.528 V and reductant potential in alkaline medium- less – 1.148 V. Current-potential curves for oxygen electrodes based on RGO, obtained by using the oxidants $K_2Cr_2O_7$, $KMnO_4$ and the reductants NaH_2PO_2, Na_2SO_3, were analyzed. The electrochemical characteristics of RGO in the oxygen reduction reaction were depended on the redox power of the reagents. We demonstrated that obtained RGO could be promising material for oxygen electrodes of fuel cells.

Cite This Article: M.O. Danilov, I.A. Slobodyanyuk, I.A. Rusetskii, G.I. Dovbeshko, and G.Ya. Kolbasov, "Influence of the synthesis conditions of reduced graphene oxide on the electrochemical characteristics of the oxygen electrode." *Nanoscience and Nanotechnology Research*, vol. 2, no. 1 (2014): 12-17. doi: 10.12691/nnr-2-1-3.

1. Introduction

An application of air or oxygen electrode in device generating electrical energy is useful, it does not give rise to environmental problems and allows saving nonrenewable natural resources. Air and oxygen electrode is a three-phase electrode-electrolyte-gas system, where the generation of electric current is localized at the phase boundary. The current magnitude generated at such gas diffusion electrode depends on the triple contact zone of these three phases. In its turn, the electrode itself is composed of catalyst and carrier. The interaction between them determines the quantity of generated current, which depends on catalyst being used. It is known that nowadays the most effective catalyst for oxygen recovering is platinum, which is a very expensive material. A great number of works is oriented towards the investigation of other effective but less costly catalysts [1]. Another problem is catalytically active and stable carrier. In works [2,3,4] the benefits of carbon nanotubes used as the carrier are shown. At present time owing to the appearance of the new nanocarbon material graphene a series of works were dedicated to its studying as an electrode material for lithium-ionic accumulators [5] and also as a catalyst carrier for catalysts in fuel cells [6-10].

At the moment the following methods of synthesis graphene from carbon nanotubes are known: intercalation of alkaline earth elements [11,12] and nitrogen [13]; plasma etching [14,15,16]; microwave unzipping [17,18];

unzipping by catalytic metal nanoparticles [19,20]; ultrasonic unzipping [21,22]; opening-up by laser irradiation [23]; electrical unzipping [24]; hydrogenating at the high-temperature [25]; unzipping by influence of a scanning tunneling microscope [26]; electrochemical unrolling [27]; the redox chemical synthesis [28,29].

The chemical methods for the preparation of graphenes involve the stages of preparation graphene oxide (GO) and its subsequent reduction to give the so-called reduced graphene oxide (RGO). Synthesis, structure and chemical properties of GO and RGO were systematized and described in detail in reviews [28,30,31].

In view of this, the study of the dependence of electrochemical properties on the method for the preparation of RGO from multi wall carbon nanotubes (MWCNTs), which is used as a catalyst support for fuel cell oxygen electrodes, is of great interest.

2. Materials and Methods

As a precursor were selected MWCNTs with hard structure of graphene layers, which leads to a decrease in the binding energy between the carbon atoms in the graphene layer. Using a suitable oxidant, one cans longitudinally "unzipping" nanotubes to form GO nanoribbons and then obtain RGO by action with a reductant.

The outer diameter of MWCNTs was about 10-40 nm, the specific surface area was 230 m^2g^{-1}, with a bulk

density of 25-35 g dm^{-3}. The number of walls was from 2-15. MWCNTs were purified of catalyst by means of hydrofluoric acid treatment.

The samples of RGO obtained by synthesis examined with the aid of a JEM-100 CXII electron microscope. The resulting synthesis RGO samples examined with an electron microscope JEM-100 CXII.The X-ray phase analysis was performed with the aid of a DRON-4 X-ray diffractometer with CuK$_\alpha$ radiation. Raman spectra of initial MWCNTs and MWCNTs after treatment were registered by inVia Raman microscope (Renishaw) under the excitation of He-Ne laser with λ_{ex} = 0.6328 Å. The position of referent Si sample at 520 cm^{-1} was used as the reference for wavenumber calibration. WiRE3.4 software was used for Raman data acquisition and data analysis.

The synthesized materials were prepared by pressing two-layer oxygen electrodes. The hydrophobic layer contained 0.07 g/cm^2 acetylene black with 25% polytetrafluoroethylene, and the active layer contained 0.02 g/cm^2 RGO, with 5% polytetrafluoroethylene. The investigations were carried out on a fuel cell mockup, a zinc electrode being used as the anode. A mockup for the testing of gas-diffusion electrodes is described in [32]. The electrolyte was a solution of 6 M KOH. A silver-chloride electrode connected through a salt bridge was used as a reference electrode. The electrochemical characteristics were recorded under galvanostatic conditions. The oxygen source was a U-shaped electrolyzer with alkaline electrolyte. Oxygen was supplied to the gas electrodes under an excess pressure of 0.01 MPa. Before measurements, the oxygen electrode was blown through with oxygen for an hour.

Platinum is deposited by electrochemical method from an aqueous solution containing 3% H$_2$PtCl$_6$ and 0.2% lead acetate (II) at a voltage of 1 V for 2 minutes, the current direction is changed through 30 s.

3. Results and Discussion

Based on the standard redox potentials of carbon [33] (Table 1) the required oxidant potential in acid medium should be more + 0.528 V and oxidant potential in alkaline medium should be more – 0.603 V.

Table 1. Oxidation potentials of carbon in different media

acidic		alkaline	
C, H$^+$ / CH$_3$OH	-0.32 V	C / CH$_3$OH, OH	-1.48 V
HCHO$_2$, H$^+$ / C	+0.528 V	CHO^{2-} / C, OH$^-$	-0.603 V
CO, H$^+$ / C	+0.518 V	CO$_3^{2-}$ / C, OH$^-$	-0.766 V
H$_2$CO$_3$, H$^+$ / C	+0.207 V		

The most famous strong oxidants (pH < 7 / pH > 7) are KMnO$_4$ (+1.69 V / +0.588 V); ozone (+2.075 V / +1.247 V); Cr$_2$O$_7^{2-}$ (+1.36 V / —)); OsO$_4$ (+1.02 V / +0.17 V); FeO$_4^{2-}$ (+2.07 V / +0.8 V), as well as several others [33].

However, if the process of breaking carbon bonds in nanotubes due to kinetic constraints, then the use of the thermodynamic redox scale for this process is not applicable.

Table 2. Oxidation potentials of carbon in different media

acidic		alkaline	
C/CH$_3$OH, OH$^-$	-1.148 V	C,H$^+$/ CH$_3$OH	-0.32 V
CHO^{2-} / C, OH$^-$	-0.603 V	HCHO$_2$, H$^+$ / C	+0.528 V
CO$_3^{2-}$ / C, OH$^-$	-0.766 V	H$_2$CO$_3$, H$^+$ / C	+0.27 V

Accordingly, for the reduced of graphene oxide in alkaline medium should be used reducing agents, with

potentials more less than -1.148 V (Table 2). In an acidic environment to reduced graphene oxide should be used reducing agents, with potentials more less than -0.320 V.

For the oxidation of MWCNTs in the acidic environment were used such oxidant as KMnO$_4$ (+1.69 V) and K$_2$Cr$_2$O$_7$ (+1.36 V). As reducing agents in an alkaline medium were used the solutions of sodium hypophosphite ($E^\ominus$ = -1.51 V) and sodium sulfite ($E^\ominus$ = -0.936 V) [33]. The method of synthesis RGO with using KMnO$_4$ is described in [34].

One gram of MCNTs was dispersed for 1 h by stirring in 30 mL of concentrated sulfuric acid. Then 10 g K$_2$Cr$_2$O$_7$ was added under stirring for 72 h at a temperature of not over 21°C. Then the diluted mixture was filtered on a fine paper filter. The precipitate was washed with hydrochloric acid (10%) and distilled water. Reduction of the oxidized product was done by similar manner [34].

Figure 1 – Figure 2 shows micrographs of RGO, reduced by sodium sulfite (Figure 1) and sodium hypophosphite (Figure 2) from the GO obtained by oxidation of MWCNTs using potassium permanganate. Figure 3 shows the XRD analysis of products obtained by reduction of sodium hypophosphite (curve H-RGO) and sodium sulfite (curve S-RGO).
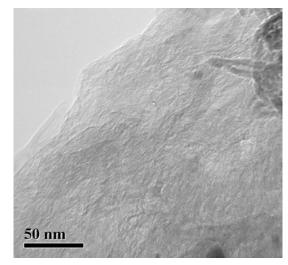

Figure 1. Micrograph of a sample of RGO obtained from MWCNTs oxidized by KMnO$_4$ and reduced with sodium sulfite
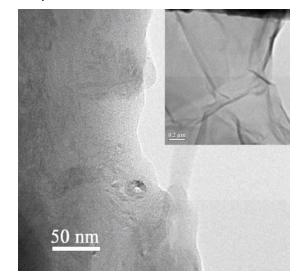

Figure 2. Micrograph of a sample of RGO obtained from MWCNTs oxidized by KMnO$_4$ and reduced with sodium hypophosphite

The XRD analysis showed the presence of two peaks, one of which corresponds to the reflection from the interplanar spacing between the graphene layers and is located at $2\theta = 25.6°$, and the second near $2\theta = 21°$ corresponds to SiO_2 (substrate). Distance between the planes in graphene is found to be 3.43 Å, which is larger than the distance between planes in graphite (3.35 Å).
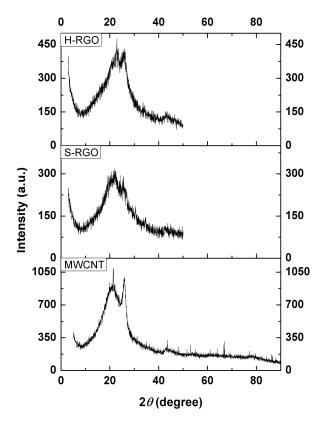

Figure 3. X-ray diagram of samples of graphene oxide reduced: (H-RGO) with sodium hypophosphite, (S-RGO) with sodium sulfite, (MWCNT) initial MWCNTs
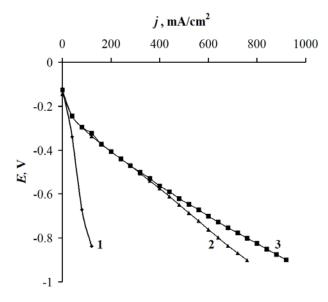

Figure 4. Dependence of potential on current density for oxygen electrodes with the active layer in an amount of 0.02 g/cm^2 consisting of initial MWCNTs (1) and RGO which were reduced by the sodium hypophosphite from MWCNTs oxidized with potassium dichromate (2) and potassium permanganate (3)

Results obtained were analyzed using *Bragg-Wolf equation* given in [35]. The initial carbon nanotubes and

samples of synthesized RGO have similar reflections; in the case of RGO reflection at $2\theta = 25.6°$ becomes wider, the crystallinity of the RGO sample deteriorates, which indicates a decrease in the size of particles. Figure 4 shows plots of potential against current density for oxygen electrodes based on RGO reduced with sodium hypophosphite from the MWCNTs oxidized by using $K_2Cr_2O_7$ (RGO-Cr) (curve 2 in Figure 4) and MWCNTs oxidized by using potassium permanganate (RGO-Mn) (curve 3 in Figure 4).

As can be seen from the current-voltage curves (Figure 4), electrodes based on RGO-Mn have better characteristics than the electrodes based on RGO-Cr. Consequently, the electrochemical properties of oxygen electrodes correlated with the oxidizing power of oxidants used.
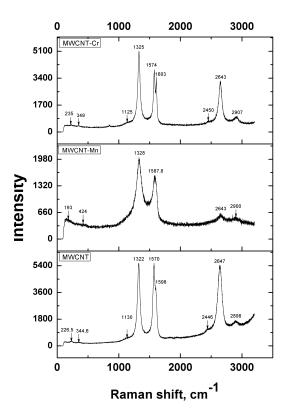

Figure 5. Raman spectra obtained at 633 nm and the intensity of 50% for initial MWCNTs (MWCNT) and RGO reduced by sodium hypophosphite from the nanotubes oxidized with potassium dichromate (MWCNT – Cr) and potassium permanganate (MWCNT – Mn)

The main feature of Raman spectra (Figure 5) of graphite structure is a so-called G band (1600 cm^{-1}) with E_{1g} symmetry in the Γ point of the Brillouin zone [36] that correlates with the ordering of graphite crystal lattice. The second feature of graphite-like materials is a D band that characterizes the disorder of graphene layer lattice [37], [38] and refers to breathing vibrations of rings of graphene layer in the K point of Brillouin zone. The second order mode of this vibration (2D band) is registered at 2600–2700 cm^{-1}, and it has an intensity which usually exceeds that of the second order vibrations and manifests a strong electron-phonon interaction. The characteristic feature of Raman spectra of MWCNT is the halfwidth equal to 50 cm^{-1} for G-mode and above 60 cm^{-1} for D-mode as well as D/G intensity ratio more than one, on the high- frequency wing of G mode one could register D′ mode [39] also. Raman spectrum of graphene monolayer

contains G and 2D bands and does not contain D mode similar to graphite, intensity of 2D mode more than G mode. Raman spectrum of graphene nanoparticles contains G, D and 2D bands analogously to MWCNT. Position of the 2D band maximum could be used as a characteristic for determination the number of layers in the graphene sheets [38,39].

Initial MWCNT has D-mode at 1322 cm^{-1}, 2D-mode at 2647 cm^{-1}, G-mode consists of 2 modes: at 1570 cm^{-1} and, so-called, D'-mode at 1598 cm^{-1}; the mode near 1130 cm^{-1} and breathing modes at 226.5, 344,6 cm^{-1}. After treatment with $KMnO_4$ ($K_2Cr_2O_7$), the spectra changed and breathing modes located at 193 and 424 cm^{-1} (235 and 349 cm^{-1}), correspondently, that should be the feature of non-homogeneity of the carbon nanotubes bungle or changes after treatment, however, the first supposition is better. After treatment with $KMnO_4$, the G and D modes became wider, and G-mode consists from one mode at 1587 cm^{-1} and D-mode at 1328 cm^{-1}, the intensity of D-mode more than G-mode, number of defects became more and electron-phonon interaction became less, intensity of 2D-mode is small and anharmonicity became more. In initial MWCNT the value of anharmonicity is equaled to 3 cm^{-1}, in MWCNT-Mn - 13 cm^{-1}. Based on the spectra analysis, a size of particles became less after treatment with $KMnO_4$, than in initial samples. After treatment with $K_2Cr_2O_7$, changes the initial nanotubes are less than after treatment with $KMnO_4$. The spectra of the MWCNT-Cr looks similar to spectra of initial MWCNT with additional defects, however, a number of defects is less than in the case of MVCNT-Mn, the intensity of D-mode became more than those for G-mode, the intensity of 2D-mode is less than in the case of initial MWCNT and, the anharmonicity of 2D mode – 7 cm^{-1}, more than in the case of initial nanotubes (3 cm^{-1}) and less than in MWCNT after treatment with $KMnO_4$ (13 cm^{-1}). Estimation of size of particles from Raman spectra (ratio D/G at λ= 632.8 nm) according to [40] gives 38.5 nm for initial MWCNT. The size for RGO reduced with sodium hypophosphite from the MWCNTs oxidized by using $K_2Cr_2O_7$ (Cr-MWCNT), is equaled to 29.6 nm. For RGO reduced with sodium hypophosphite from the MWCNTs oxidized by using potassium permanganate (RGO-Mn) we got a size equaled to 27.5 nm. These results were obtained with formulae taken from [40]:

$$L_a\left(nm\right)=\frac{560}{E_l^4}\left(\frac{I_D}{I_G}\right)^{-1},$$

where *La* is the crystallite sizes, E_l is the excitation energy used in the Raman experiment in eV, I_D and I_G intensity of the *D* and *G* modes, respectively.

After the oxidizing with potassium permanganate, the surface of nanotubes undergo to oxidation better than in the case of oxidizing with $K_2Cr_2O_7$. In the case of exposure of MWCNT by HNO_3, the surface of nanotubes became drastic disordered [41]. Our oxidants are stronger than HNO_3. So we suppose that after treatment by oxidizing with potassium permanganate, the MWCNT became more defective and disordered, Raman spectra drastically changed and looks like the amorphous carbon. The last fact lead to better longitudinal (sometimes transverse) breaks of carbon nanotubes, and as result, outer layers come off and their unzipping occur. We suppose that after

treatment with potassium permanganate, initial MWCNT undergoes more changes in structure that those for $K_2Cr_2O_7$, the numbers of defects became more, sizes of particles became less and nanotubes seems to unzip better than in the case of oxidation of $K_2Cr_2O_7$, number of layers are equaled to those in carbon nanotubes or less.

Figure 6 shows plots of potential against current density for oxygen electrodes based on RGO obtained from the MWCNTs oxidized by potassium permanganate followed by reduction this product with sodium sulfite (curve 2) (RGO-SS) and sodium hypophosphite (curve 3) (RGO-SH).
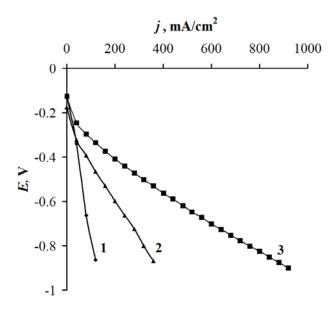

Figure 6. Dependence of potential on current density for oxygen electrodes with the active layer in an amount of 0.02 g/cm^2 consisting of initial MWCNTs (1) and MWCNTs oxidized with potassium permanganate which were reduced to RGO with sodium sulfite (2) and sodium hypophosphite (3)
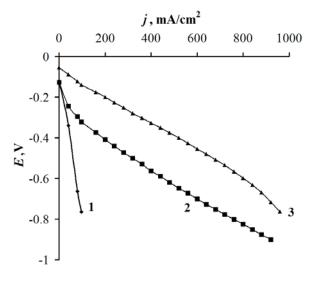

Figure 7. Dependence of potential on current density for oxygen electrodes with the active layer in an amount of 0.02 g/cm^2 consisting of initial MWCNTs (1), RGO obtained by the reduction of sodium hypophosphite MWCNTs oxidized with potassium permanganate (2), MWCNTs with deposited metallic platinum in an amount of 10 wt%

As can be seen (Figure 6), the electrodes based on RGO-SH at the same potential have large currents than the electrodes based on RGO-SS. Consequently, the electrochemical properties of the oxygen electrode

correlated with a reduction power of the reducing agent. It should be noted that the standard redox potential of sodium sulfite in an alkaline medium среде ($E^{\ominus}$ = -0.936 V) more positive than required, in our view, the reduction potential of the GO in an alkaline medium $E^{\ominus}$ = -1.148 V. We can assume that sodium sulfite partially reduced some carboxy groups the reduction potential which is more than -0.936 V. In our opinion, this leads to a difference in the characteristics of the oxygen electrodes based on RGO-SS.

Figure 7 shows the comparative characteristics of the oxygen electrodes based on synthesized RGO and MWCNTs with deposited platinum.

As can be seen from the Figure 7, electrodes based on RGO-SH in their electrocatalytic characteristics approaching to electrodes based on carbon materials with deposited platinum. Oxygen electrodes based on reduced graphene oxide in galvanostatic mode were stable for six months at a current density 200 mA/cm^2.

4. Conclusions

We showed that a choice of oxidizing and reducing agents for the synthesis of reduced graphene oxide from multi-walled carbon nanotubes could be done on the basis of standard redox potentials. We found and concluded that the obtained reduced graphene oxide is a promising carrier of catalysts for the oxygen fuel cell electrode, which can replace the commercial electrode materials containing platinum.

References

[1] Bidault, F., Brett, D.J.L., Middleton, P.H., Brandon, N.P., "Review of gas diffusion cathodes for alkaline fuel cells," *J Power Sources*, 187 (1). 39-48. 2009.

[2] Soehn, M., Lebert, M., Wirth, T., Hofmann, S., Nicoloso, N., "Design of gas diffusion electrodes using nanocarbon," *J Power Sources,* 176 (2). 494-498. 2008.

[3] Hsieh, C-T., Lin, J-Yi., Wei, J-L., "Deposition and electrochemical activity of Pt-based bimetallic nanocatalysts on carbon nanotube electrodes," *Int J Hydrogen Energy*, 34 (2). 685-693. 2009.

[4] Wang, X., Waje, M., Yan, Y., "CNT-Based Electrodes with High Efficiency for PEMFCs," *Electrochem Solid-State Lett*, 8 (1). A42-A44. 2005.

[5] Wang, G., Shen, X., Yao, J., Park, J., "Graphene nanosheets for enhanced lithium storage in lithium ion batteries," *Carbon*, 47 (8). 2049-2053. 2009.

[6] Xin, Y., Liu, J., Jie, X., Liu, W., Liu, F., Yin, Y., Gu, J., Zou, Z., "Preparation and electrochemical characterization of nitrogen doped graphene by microwave as supporting materials for fuel cell catalysts," *Electrochimica Acta*, 60. 354-358. 2012.

[7] Lin, Z., Waller, G,, Liu, Y., Liu, M., Wong, C.P., "Facile synthesis of nitrogen-doped graphene via pyrolysis of graphene oxide and urea and its electrocatalytic activity toward oxygen reduction reaction," *Adv Energy Mater*, 2 (7). 884-888. 2012.

[8] Qu, L.T., Liu, Y., Baek, J.B., Dai, L.M., "Nitrogen-doped graphene as efficient metal-free electrocatalyst for oxygen reduction in fuel cells," *ACS Nano* 4. 1321-1326. 2010.

[9] Lin, Z.Y., Song, M.K., Ding, Y., Liu, Y., Liu, M.L., Wong, C.P., "Facile preparation of nitrogen-doped graphene as a metal-free catalyst for oxygen reduction reaction," *Phys Chem Chem Phys,* 14. 3381-3387. 2012.

[10] Shao, Y., Zhang, S., Wang, C., Nie, Z., Liu, J., Wang, Y., Lin, Y., "Highly durable graphene nanoplatelets supported Pt nanocatalysts for oxygen reduction," *J Power Sources,* 195. 4600-4605. 2010.

[11] Cano-Márquez, A.G., Rodriguez-Macias, F.J., Campos-Delgado, J., et al., "Ex-MWNTs: Graphene sheets and ribbons produced by lithium intercalation and exfoliation of carbon nanotubes," *Nano Lett,* 9. 1527-1533. 2009.

[12] Kosynkin, D.V., Lu, W., Sinitskii, A., Pera, G., Sun, Z., Tour, J.M., "Highly conductive grapheme nanoribbons by longitudinal splitting of carbon nanotubes using potassium vapor," *ACS Nano*, 5. 968-974. 2011.

[13] Morelos-Gómez, A., Vega-Díaz, S.M., González, V.J., et al, "Clean nanotube unzipping by abrupt thermal expansion of molecular nitrogen: graphene nanoribbons with atomically smooth edges," *ACS Nano,* 6. 2261-2272. 2012.

[14] Jiao, L., Zhang, L., Wang, X., Diankov, G., Dai, H., "Narrow graphene nanoribbons from carbon nanotubes," *Nature,* 458. 877-880. 2009.

[15] Valentini, L., "Formation of unzipped carbon nanotubes by CF$_4$ plasma treatment," *Diamond & Related Materials*, 20. 445-448. 2011.

[16] Mohammadi, S., Kolahdouz, Z., Darbari, S., Mohajerzadeh, S., Masoumi, N., "Graphene formation by unzipping carbon nanotubes using a sequential plasma assisted processing," *Carbon,* 52. 451-463. 2013.

[17] Janowska, I., Ersen, O., Jacob, T., et al, "Catalytic unzipping of carbon nanotubes to few-layer graphene sheets under microwaves irradiation," *Appl Catal A*, 371. 22-30. 2009.

[18] Vadahanambi, S., Jung, J-H., Kumar, R., Kim, H-J., Oh, I-K., "An ionic liquid-assisted method for splitting carbon nanotubes to produce graphene nano-ribbons by microwave radiation," *Carbon,* 53. 391-398. 2013.

[19] Elías, A.L., Botello-Méndez, As.R., Meneses-Rodríguez, D., et al, "Longitudinal cutting of pure and doped carbon nanotubes to form graphitic nanoribbons using metal clusters as nanoscalpels," *Nano Lett,* 10. 366-372. 2009.

[20] Parashar, U.K., Bhandari, S., Srivastava, R.K., Jariwala, D., Srivastava, A., "Single step synthesis of graphene nanoribbons by catalyst particle size dependent cutting of multiwalled carbon nanotubes," *Nanoscale,* 3. 3876-3882. 2011.

[21] Jiao, L., Wang, X., Diankov, G., Wang, H., Dai, H., "Facile synthesis of high-quality graphene nanoribbons," *Nat Nanotechnol,* 5. 321-325. 2010.

[22] Xie, L., Wang, H., Jin, C., et al1, "Graphene nanoribbons from unzipped carbon nanotubes: Atomic structures, Raman spectroscopy, and electrical properties," *J Am Chem Soc,* 133. 10394-10397. 2011.

[23] Kumar, P., Panchakarla, L.S., Rao, C.N.R., "Laser-induced unzipping of carbon nanotubes to yield graphene nanoribbons," *Nanoscale,* 3. 2127-2129. 2011.

[24] Kim, K., Sussman, A., Zettl, A., "Graphene nanoribbons obtained by electrically unwrapping carbon nanotubes," *ACS Nano,* 4. 1362-1366. 2010.

[25] Talyzin, A.V., Luzan, S., Anoshkin, I.V., et al, "Hydrogenation, purification, and unzipping of carbon nanotubes by reaction with molecular hydrogen: Road to graphane nanoribbons," *ACS Nano,* 5. 5132-5140. 2011.

[26] Pavia, M.C., Xu, W., Proenca, M.F., Novais, R.M., Laegsgaard, E., Besenbacher, F., "Unzipping of functionalized multiwall carbon nanotubes induced by STM," *Nano Lett,* 10. 1764-1768. 2010.

[27] Shinde, D.B., Debgupta, J., Kushwaha, A., Aslam, M., Pillai, V.K., "Electrochemical unzipping of multi-walled carbon nanotubes for facile synthesis of high-quality graphene nanoribbons," *J Am Chem Soc,* 133. 4168-4171. 2011.

[28] Kosynkin, D.V., Higginbotham, A.L., Sinitskii, A., et al, "Longitudinal unzipping of carbon nanotubes to form graphene nanoribbons," *Nature,* 458. 872-876. 2009.

[29] Zhang, S., Zhu, L., Song, H., et al, "How graphene is exfoliated from graphitic materials: synergistic effect of oxidation and intercalation processes in open, semi-closed, and closed carbon systems," *J Mater Chem,* 22. 22150-22154. 2012.

[30] Zhu, Y., Murali, S., Cai, W., et al, "Graphene and graphene oxide: Synthesis, properties, and applications," *Adv Mater,* 22. 3906-3924. 2010.

[31] Pei, S., Cheng, H.-M., "The reduction of graphene oxide," *Carbon,* 50. 3210-3228. 2012.

[32] Danilov, M.O., Kolbasov, G.Ya., Rusetskii, I.A., Slobodyanyuk, I.A., "Electrocatalytic properties of multiwalled carbon nanotubes-based nanocomposites for oxygen electrodes," *Russian J Appl Chem,* 85. 1536-1540. 2012.

[33] Bratsch, S.G., "Standard electrode potentials and temperature coefficients in water at 298.15 K," *J Phys Chem,* 18. 1-21. 1989.

[34] Danilov, M.O., Slobodyanyuk, I.A., Rusetskii, I.A., Kolbasov, G.Ya., "Reduced graphene oxide: a promising electrode material for oxygen electrodes," *J Nanostructure Chemistry*, 3:49. 2013.

[35] Kittel, Ch., *Introduction to Solid State Physic,* Wiley, 8th Edition. 2004.

[36] Nemanich, R.J., Solin, S.A., "Observation of an anomolously sharp feature in the 2nd order Raman spectrum of graphite," *Solid State Comm,* 23. 417-420. 1977.

[37] Nemanich, R., Solin, S., "First-and second-order Raman scattering from finite-size crystals of graphite," *Phys Rev B*, 20. 392-401. 1979.

[38] Vidano, R., Fishbach, D., "Observation of Raman band shifting with excitation wavelength for carbons and graphites," *Solid State Comm,* 39. 341-344. 1981.

[39] Ferrari, A., Basko, D., "Raman spectroscopy as a versatile tool for studying the properties of graphene," *Nature nanotechnology*, 8. 235-246. 2013.

[40] Cancado, L.G., Takai, K., Enoki, T., Endo, M., Kim, Y.A., Mizusaki, H., Jorio, A., Coelho, L.N., Magalhães-Paniago, R., Pimenta, M.A., "General equation for the determination of the crystallite size *La* of nanographite by Raman spectroscopy," *Appl. Phys.Lett.,* 88163106. 2006.

[41] Yanchuk, I.B., Koval′s′ka, E.O., Brichka, A.V., Brichka, S.Ya., "Raman scattering studies of the influence of thermal treatment of multi-walled carbon nanotubes on their structural characteristics," *Ukr. J. Phys.,* 54. 407-412. 2009.